Spatial Ecological Patterns in Health-compromised *Porites* Corals

by

Bryant William Grady

A Thesis Presented in Partial Fulfillment
of the Requirements for the Degree
Master of Arts

Approved March 2022 by the
Graduate Supervisory Committee:

Gregory Asner, Chair
Stewart Fotheringham
Mary Donovan
John Burns

ARIZONA STATE UNIVERSITY

May 2022

ABSTRACT

Coral diseases have become a major vector of change in coral reef physical architecture, functional ecology, and community structure. While the field of spatial community characteristics and coral disease research is growing, major gaps exist in the combination of the two areas of study. Here, I visually assessed over 100,000 massive *Porites* corals across 41 reefs in South Kona, Hawaii to investigate the spatial ecology of visually compromised corals. These corals were assessed for seven specific health conditions common to the region: algal infection, pigmentation response, algal overgrowth, *Ramicrusta* infection, skeletal growth anomalies, *Porites* trematodiasis, and tissue loss syndrome. Only 6.6% of corals surveyed exhibited a compromised health state and overall condition severity was low; less than 10%. Attributes representing colony assemblage structure showed few observed patterns with the severity and prevalence of these coral health conditions. Additional findings revealed that coral colony traits such as perimeter length had a positive effect on the presence of seven different coral health conditions. Whereas the interaction of both increasing colony surface area and perimeter length was negatively associated the presence of the health conditions. By using global and local spatial statistics, I uncovered trends in reefscape- and colony-level spatial patterns of health-compromised corals. Significant spatial structure existed among colonies based on their health condition severity. However, I found infrequent non-random spatial patterns in most reefs in South Kona.

DEDICATION

To the amazing people of South Kona for allowing me to study their amazing reefs and conduct field work, my friends and family who supported me throughout this process, a superb fleet of volunteers who assisted in coral annotations and coral health surveys for without their help this study would not have been possible, and to a particularly charismatic group of elders who answered my questions regularly.

TABLE OF CONTENTS

LIST OF TABLES

LIST OF FIGURES

Introduction

Coral diseases have caused changes to coral reefs globally (Young et al., 2020; Harvell et al., 2007; Patterson et al 2002; Richardson et al., 1998). Diseases afflicting corals have been observed worldwide, but for many, what causes them and how they spread across reefscapes is still unknown (Aeby 2015; Harvell et al., 2007; Thurber et al., 2020). Major areas of disease prevalence, and thus disease research, have occurred in the Caribbean, Hawaii, and the Indo-Pacific (Aeby et al., 2011; Ruiz-Moreno et al., 2012; Harvell et al., 2007). Unlike coral bleaching events or storm damage, snap events that cause major damage over a short period (Pascoe et al., 2021), coral disease is an active form of reef decay that can degrade reefs over the long term (Maynard et al., 2015).

Despite a multitude of studies in laboratory and field settings, only a handful of the pathogens, bacteria, or viruses that cause certain diseases have been identified (Thurber et al., 2020; Work and Meteyer 2014). However, over the past several decades, studies measuring drivers and processes that influence coral disease have been widely implemented (Caldwell et al., 2020; Caldwell et al., 2016; Aeby 2015; Couch et al., 2014; Harvell et al., 2007). Local stressors have been found to exacerbate the prevalence and severity of existing coral disease (Magel et al., 2019; Sheridan et al., 2014; Burns et al., 2011). For example, increased sedimentation (Harvell et al., 2007), coastal development (Caldwell et al., 2020, Burns et al., 2011), excess nutrients (Yoshioka et al., 2016), and marine heat waves (Maynard et al., 2015) have been shown to influence coral disease prevalence and severity. In a study from the Caribbean, corals that experienced bleaching had a 51-times higher rate of disease than pre-bleaching disease levels (Miller et al., 2019). The continuation of marine heatwaves and coral bleaching events is predicted to increase the severity of coral disease worldwide

independent of local stressors; causing coral disease to become as great of a threat to reef decline as coral bleaching by 2050 (Maynard et al., 2015; Ward et al; 2007).

Over the past several decades, field assessment surveys have been the most prominent way of assessing and studying coral disease (Montilla et al., 2019). Field investigations have focused on establishing the distribution and demographics of diseased corals (Aeby et al., 2011; Burns et al., 2020; Couch et al., 2021; Couch et al., 2014; Muller et al., 2020; Nicolet et al., 2017). Disease assessment studies use a diver-based approach to 1) identify the number and size of colonies, 2) identify the presence/absence of a given or multiple diseases, and 3) determine the severity and extent of diseased or afflicted tissue on each colony (Caldwell et al., 2016; Couch et al., 2021; Winston et al 2018; Walsh et al., 2013). More recent advancements in survey methods and technology allow for fine-scale remote sensing (< 1 m resolution) and Structure from Motion (SfM) surveys (< 1 cm resolution) to advance and accelerate coral reef assessments and *in-situ* surveys (Couch et al., 2021; Bayley and Mogg 2020; Pederson et al., 2019; Fox et al., 2019; Edwards et al., 2017; Ferrari et al., 2017; Bryson et al., 2017).

Evolving methodologies to collect coral community and coral health data have been used to quantify specific coral colony metrics such as surface area, perimeter length, colony diameter, growth rates, and spatial patterns of coral species and morphologies (Sandin et al., 2021; Pederson et al., 2019; Burns et al., 2015). Studies have found that the accuracy of SfM surveys relative to *in-situ* diver-based methods yield comparable results, and that there may be “no gold standard” for data collection on both coral health and community composition (Burns et al., 2020; Couch et al., 2021). These new methodological techniques have created opportunities to ask more complex questions about the spatial ecology of corals and their diseases. Burns et al., (2016)

used colony-scale 3D models from SfM surveys and found that skeletal growth anomalies expressed nonrandom patterning across colony surfaces. Edwards et al., (2017) and Pederson et al., (2019) found spatial patterns of coral colonies that are taxon specific and are influenced by colony size across reefscapes. While the field of spatial community characteristics and coral disease research is growing, major gaps exist in the combination of the two areas of inquiry.

Understanding how trends of diseased corals are related to coral assemblage structure, spatial patterns of corals, and specific coral traits remains an evolving area of research. The use of spatial coral colony characteristics and coral disease data may reveal how disease is spreading among coral assemblage groups, as well as how the spatial relationship between colonies influences disease severity. As coral reefs change, inquiries investigating different assemblage structures and colony traits may provide useful information to managers and conservationists on ways to reduce or control the spread of a given health condition or infectious disease. Here, I investigate the relationship between seven specific health conditions and corals in the genus *Porites*, specifically focusing on those with massive morphologies. I ask the following questions: 1) do reefscape-scale patterns of coral density, spatial structure, and size class influence the severity and prevalence of a given coral health condition, 2) is the presence of a health condition related to coral traits such as colony perimeter and colony surface area, and 3) does spatial patterning exist among corals with more severe health conditions? The results and methods used in this study will provide insights into how health-compromised corals are distributed among assemblage patterns as wells as provide insight into how health conditions can be mapped.

Materials and Methods

Site Description

I focused on reefs located in the South Kona District of Hawaii Island, USA (Figure 1). This region has been identified as one of the most intact reef systems in terms of coral cover in the State of Hawaii (Asner et al., 2020). These reefs are dominated by coral species in the genus *Porites*, with both branching and massive morphologies. Shallow water benthic substrates are composed of basalt and igneous boulders, whereas intermediate and deeper depths have a mix of basalt spurs and calcareous reef substrates.

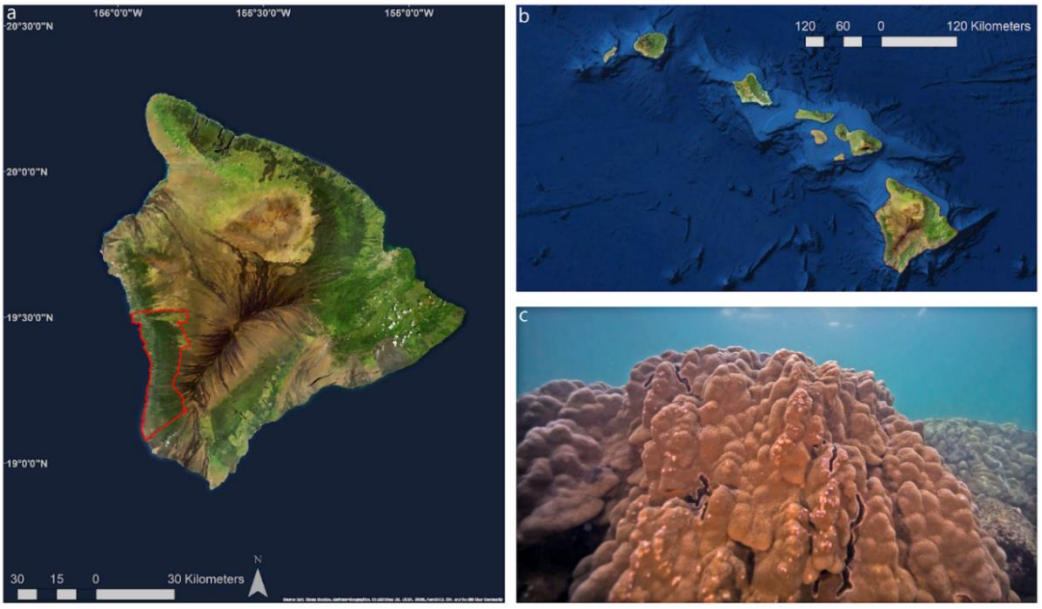

Figure 1. Map of study location (a) Hawaii island, southeastern most island in Hawaiian archipelago. South Kona Region of Hawaii Island highlighted in red, (b) State of Hawaii, and (c) a typical massive *Porites* coral colony that characterizes reefs in the study area.

Field Sampling

Initial site selection utilized sites from the annual South Kona Initiative (SKI) reef surveys (Asner et al., 2021). These surveys used a stratified random sampling process that empirically characterizes marine coastal habitats by benthic and near-shore composition (Asner et al., 2020 & 2021). This type of sampling design aimed to capture the variance that exists in reef habitat types from 0 - 18 m, while accurately capturing the habitat variance across the region. My study used the 117 sites and data collected from these surveys that took place in the months June - August 2020. A full description of the stratification and site selection method can be found in the methods section of Asner et al. (2021).

Data Analysis and Creation

At each site, I conducted a 10 m x 10 m SfM survey to generate 3D reconstructions of benthic substrates at sub-centimeter resolution. 3D reconstructions were created using Agisoft Metashape software (Version 1.7 Agisoft LLC 11 St. Petersburg, Russia, 191144) to produce spatially referenced mosaics detailing coral colonies and benthic substrates within the survey area. Methods for model and mosaic development are described in Burns et al. (2015) and Bayley and Mogg (2020). Unlike standard SfM surveys, I collected photos at an elevation of 0.25 m - 0.50 m off the benthos as opposed to the traditional 1 m elevation. By collecting photos this way, I achieved higher pixel density per cm as well as a higher picture density per point. I traced individual corals by genus and morphology type, focusing on *Porites* corals with massive morphologies (Figure 2). Colony delineations were made around colony borders using Mask R-CNN; an initial unsupervised classification technique described in Chen et al. (2019). Annotations output from the Mask R-CNN models were visually assessed and

edited when necessary in the software platform TagLab (Visual Computing Lab) (Pavoni et al., 2020). Visual assessments on Mask R-CNN annotations were for the precision and accuracy checks of model predicted annotations. When annotations did not accurately capture a colony boundary or misidentified a coral, these edits were corrected in TagLab. I converted colony delineations into shapefiles in TagLab for use in further assessments of spatial metrics and to determine individual colony surface area, diameter, and perimeter length.

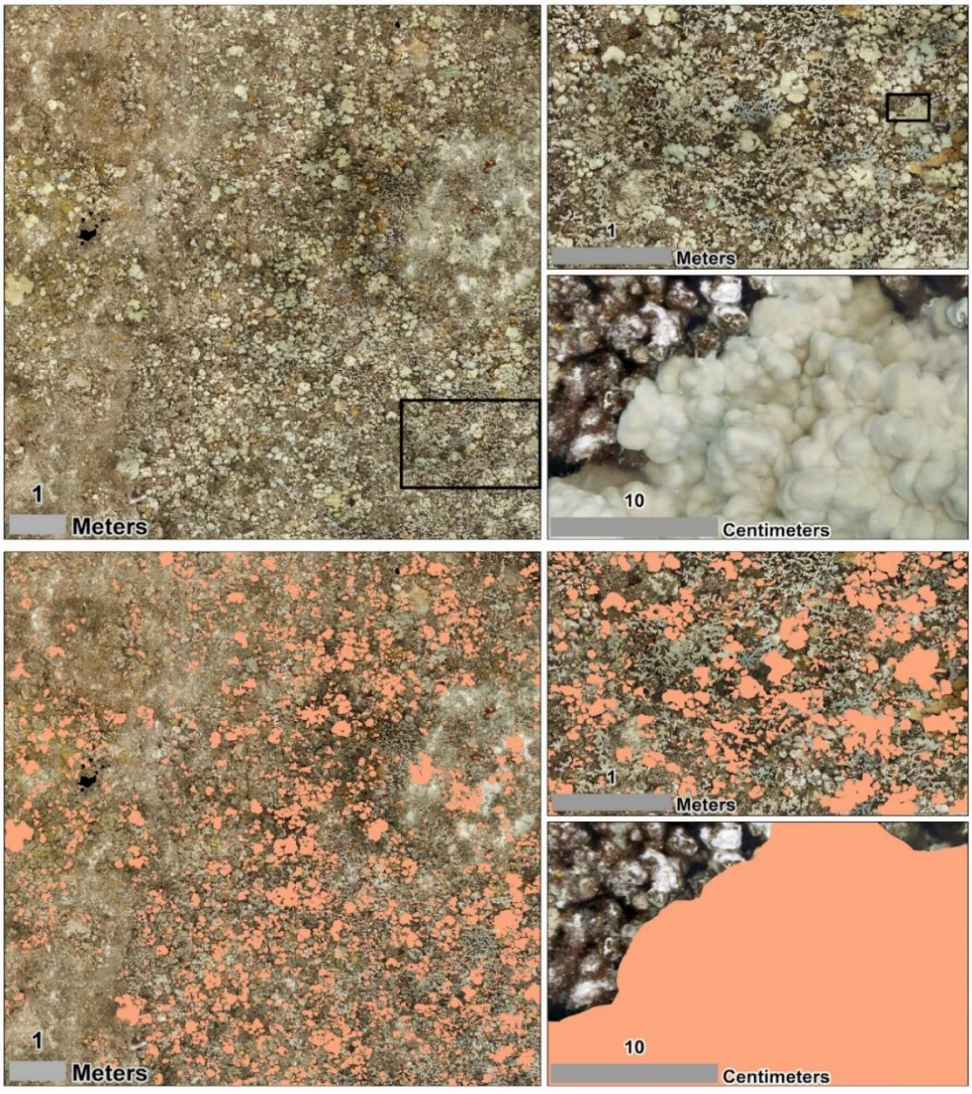

Figure 2. Mosaic maps of an example South Kona site at multiple scales (Top) and mosaic maps with cleaned Mask R-CNN massive *Porites* annotation (Bottom).

Multidimensional Latin Hypercube Sampling

Due to the extensive time requirement when conducting coral health surveys, I used quantitative approach to reduce the number of sites at which digital coral health surveys were conducted based on the variance within data. I looked at variables that describe the site-level assemblage structure of massive *Porites* colonies and used four metrics to describe assemblage structure: colony density (corals per m^2), size class diversity (H'), average colony size (m^2), and a site level spatial pattern index based on the size of colonies. A description of how these data were generated can be found in Appendix A. I used multidimensional Latin hypercube sampling to assess the variance within and between independent variables across sites. Sites that capture the variance among all sites were selected to reduce the number of redundant sites that have the same assemblage structure. The process for this sampling uses binning based on percentiles of the assemblage variables. I used three bins assessing the 0 - 33, 33 - 66, and 66 - 100th percentile of each variable. For each combination of binned variables, a single site was selected at random from the sites that fell into that bin (McKay et al., 2000). By conducting my analysis in this manner, I reduced the sites and therefore time it took to conduct coral health sampling while capturing the variance that exists spatially and ecologically within these assemblage structure variables and study region.

Coral Health Surveys

Burns et al., (2020) and Couch et al., (2021) found that both coral community surveys and coral health surveys yield comparable results when diagnostically comparing *in-situ* diver-based methods to digital SfM mosaic surveys. My coral health surveys used these new digital methods and focused on massive *Porites* annotations from the reduced

number of sites. Because the cause of many diseases has yet to be determined, the difference between what constitutes a compromised health state and a disease remains vague. Thus, for the purposes of this study, I will refer to “diseased” and “health-compromised corals” as those with “health conditions”. For each site, I assessed *Porites* colonies for seven health conditions: Algal infection (ALG), pigmentation response (PRS), algal overgrowth (ALOG), *Ramicrusta* infection (RAMI), skeletal growth anomalies (SGA), *Porites* trematodiasis (PTR), and tissue loss syndrome (TLS) (Figure 3). Coral health surveys were linked to individual coral shapefile polygons to map health conditions directly to mosaic annotations (Supplementary Figure 1). These health conditions were selected due to their prevalence in South Kona as well as use in past coral health surveys (Couch et al., 2014). *Ramicrusta* Infection is new to coral health surveys in Hawaii due to the discovery of *Ramicrusta hawaiiensis* in the archipelago in 2021 (Sherwood et al ., 2021), as well as its newly found distribution across South Kona (Grady et al., in prep). A full description of each health condition is in Appendix A. My assessment of each colony included the presence/absence of each health condition as well as the severity of those present. Prior to coral health surveys, surveyors were calibrated using pre-annotated colonies to minimize surveyor bias. All coral health surveys were analyzed in ArcMap GIS (Version 10.7.1 Environmental Systems Research Institute, Inc.) in conjunction with Agisoft Metashape software for use of both the mosaic, 3D model, and individual images to maximize angles and determine colony health effectively.

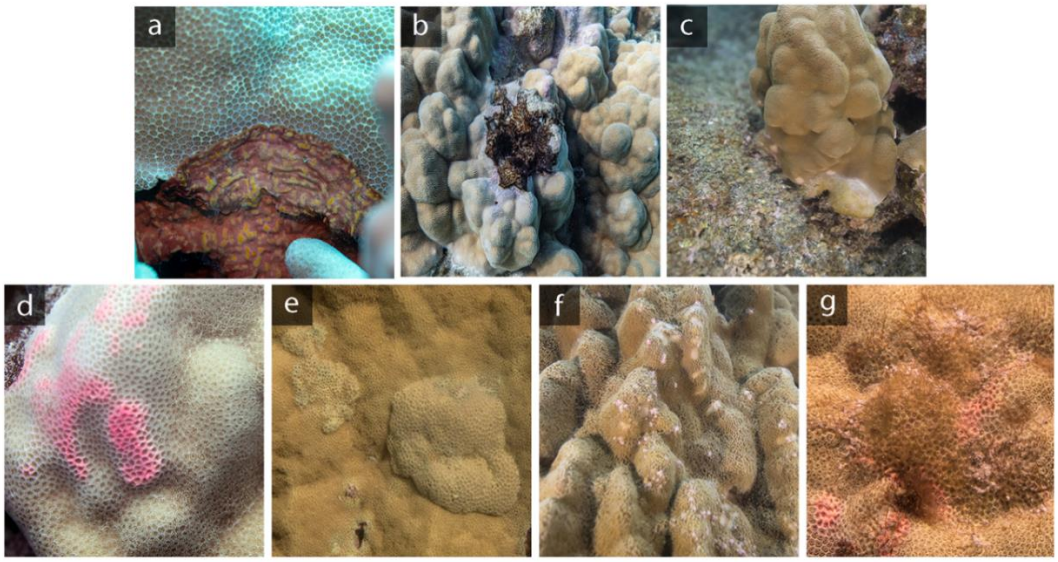

Figure 3. Images of massive *Porites* corals with different compromised health states: (a) *Ramicrusta* Infection, (b) Algal Overgrowth (image pending), (c) Tissue Loss Syndrome (image pending), (d) Pigmentation Response, (e) Skeletal Growth Anomalies, (f) *Porites* trematodiasis, and (g) Algal Infection.

Coral Health and Assemblage Statistical Analysis

To assess relationships between site level massive *Porites* assemblage structure and coral health conditions, I used an Ordinary Least Squares (OLS) regression model. Two independent response variables describing coral health condition, prevalence and proportional severity, were calculated to site level. Health condition prevalence was quantified as the number of afflicted corals per every thousand corals. Coral health severity data were transformed prior to analysis to unbound the data using a logit transformation, from data that existed between 0 and 100 to a continuous variable. The assemblage predictor variables were scaled to a mean of zero and standard deviation of one to remove units and make estimates comparable between variables. Massive *Porites* assemblage structure predictor variables included colony density, size class diversity, and a site level spatial pattern index. Predictor variables were assessed for

multicollinearity using Variation Inflation Factor (VIF) scores prior to statistical analysis. A VIF score above 5 was used as a cutoff for multicollinearity occurring between variables. No variable had a VIF score above 2, and therefore all were kept in the models. Residuals were visually inspected graphically for each model.

Coral Health and Colony Trait Statistical Analysis

To assess the relationship of colony traits with colony health data, I used Generalized Mixed Effects Models (GLMMs). For this analysis, I used each individual colony assessed during the coral health surveys as a replicate, where the presence or absence of each health condition followed a binomial distribution. Coral trait data, colony surface area, perimeter length, and the interaction between surface area and perimeter length were used as fixed effect predictor variables. Because colonies were nested within sites, and the number of colonies varied at each site, site was used as a random effect in the model. Predictor variables were scaled to a mean of zero and standard deviation of one prior to analysis. The interaction terms were assessed using a Likelihood Ratio Test (LRT) to infer if there was more information provided by assessing increases in both variables together rather than just independently.

Coral Health Reefscape and Colony Spatial Analysis

To define the spatial pattern of health-compromised corals at colony and reef scales, I used Global Moran's I indices. A Global Moran's I statistic is one of the most common ways to test for non-random spatial patterns and spatial structure (Moran 1950). Afflicted corals may exhibit spatial structuring simply because the corals at a

given site exhibit spatial structuring, so I included both health compromised and healthy colonies in the analysis. For every healthy colony, the severity value was given a 0. For each site, a Moran's I test used a site's unique *MaxdiffK* statistic as the Euclidean distance and a Gaussian weighting scheme (Appendix A). This assesses the maximum differential clustering distance within a cluster of corals at a site, weighting corals nearer to each other higher than those farther away. Each Moran's I test was compared against 199 random permutations and a pseudo p-value was calculated to compare the resulting p-value from the test to that of the 199 randomly generated spatial patterns. The I-value from each test described the spatial pattern of health compromised corals based on their severity per health condition. At sites where significant departures from randomness existed, a Getis-Ord Local statistic (GI*) was used to identify areas where health condition clusters occur among colonies (Ord and Getis 1995). Where a Global Moran's I test will indicate if a site has significant clustering or dispersion based on a health condition's severity, a Getis-Ord Local statistic will show exactly which colonies have clustering based on their condition severity and show condition hotspots. I use G values from the Getis-Ord Local statistic and individual colony shapefiles to indicate the level and intensity of the spatial pattern. I generated Individual site maps as data products to show varying levels of spatial structuring. A full schematic of the methods is located in Figure 4.

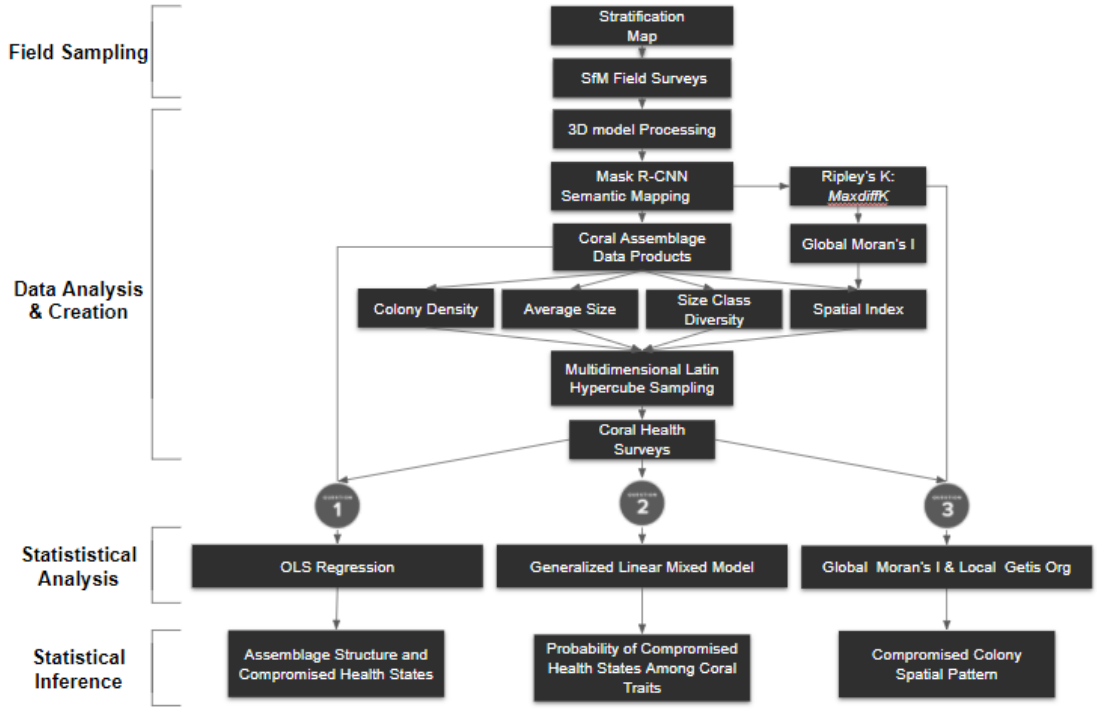

Figure 4. Schematic visualizing the workflow of site selection, field and lab surveys, data collection and development, data upscaling, analyses, and data products.

Results

South Kona Coral Health Trends

My initial site level investigation used the 117 sites from the annual South Kona Intensive reef surveys. Of these 117 sites, model alignment and mosaic construction errors occurred in six of them, with 111 successful mosaics generated. Of the remaining 111 sites, I removed an additional five sites due to benthic cover consisting of only sand with no corals present. The remaining 106 sites had 280,720 massive *Porites* colonies with an average site density and standard error of (25.7 ± 1.87 m^2), a size spatial index of and standard error (0.012 ± 0.001), diversity among sizes and standard error

measuring (1.05 ± 0.021), and an average size and standard error of (0.0034 ± 0.0002 m^2). Multidimensional Latin hypercube subsampling indicated that it was possible to reduce these 106 sites to 41 while still capturing the same variance within the study region (Supplementary Figure 2 and 3). The 41-site subset had a total of 100,098 massive *Porites* corals with an average site density and standard error of (25.7 ± 2.94 m^2), a size spatial index and standard error of (0.012 ± 0.003), diversity among sizes and standard error of (1.05 ± 0.035), and an average size and standard error of (0.0034 ± 0.0004 m^2) (Supplementary Figure 4; Supplementary Table 1).

Massive *Porites* corals were affected by all seven of the diseases and health conditions in this study. Of the 100,098 corals visually assessed, 6,667 (6.6%) colonies were in a visually compromised health state. The prevalence at which these corals health conditions occurred and their average severity are reported in Table 1. Average severity illustrates the overall health of all corals by condition and site, but it misrepresents the severity proportional to those corals that are in a compromised health state. To address this, I calculated proportional severity which is the average severity of only the colonies in a visibly compromised health state (Table 1). Health Condition prevalence was calculated by the ratio of compromised colonies to total colonies. This incident prevalence was multiplied by 1,000 to obtain the prevalence of compromised colonies per 1,000 colonies for each health condition (Table 1).

Table 1. Regional level metrics (means of site means) describing the mean severity, mean proportional severity, prevalence of health condition presence per 1000 colonies, and number of sites where present (n). Mean severity is the severity of each health condition across all corals at a site. Proportional severity is the mean of only those corals that had a given condition.

Health Condition	Mean severity %	*SE* ±	Mean Proportional severity %	*SE*±	Prevalence n^{-} ^{1000} colonies	*SE* ±	Sites present n
Algal Infection (**ALG**)	1.28	0.2	5.01	1.08	1.6	0.91	15
Pigmentation Response (**PRS**)	1.93	0.75	3.42	0.82	50.75	10.42	40
Algal Overgrowth (**ALOG**)	2.48	0.87	8.02	0.68	17.24	2.1	41
Ramicrusta Infection (**RAMI**)	0.75	0.56	5.42	0.88	7.12	1.71	24
Skeletal Growth Anomalies (**SGA**)	0.47	0.34	4.16	0.54	10.14	2.93	36
Porites Trematodiasis (**PTR**)	0.34	0.03	0.32	0.95	1.44	0.5	18
Tissue Loss Syndrome (**TLS**)	0.15	0.31	11.91	1.02	0.63	0.17	18

Coral Health and Reefscape Coral Assemblage Relationships

The OLS multiple regression models reported interesting findings regarding the relationship between the health condition proportional severity and health condition prevalence with the massive *Porites* reefscapes assemblage structure variables. Tissue loss syndrome was the only health condition to show a significant relationship with proportional severity and an assemblage variable: colony density ($R^2 = 0.24$). Skeletal Growth Anomaly was the only health condition to show relationships with condition prevalence and assemblage variables: colony density ($R^2 = 0.12$) and size class diversity ($R^2 = 0.12$). A full description of these OLS multiple regression results are available in Appendix A in Supplementary Table 2 and Table 3.

Patterns Among Coral Health and Colony Traits

The GLMMs indicated strong relationships with each of the seven health conditions for both colony perimeter length and colony surface area (Figure 5, Table 2). For algal overgrowth (ALOG), algal infection (ALG), and *Porites* trematodiasis (PTR) increases in perimeter length were associated with increased probability of these health conditions. I found that for conditions *Ramicrusta* infection (RAMI), tissue loss syndrome (TLS), pigmentation response (PRS), and skeletal growth anomalies (SGA), the

magnitude of the positive effect of perimeter length was lower compared to the other four health conditions (Figure 5). The GLMMs also indicated that surface area was a potential indicator for compromised health except for *Ramicrusta* infection and *Porites* trematodiasis. While surface area had a significant effect, it is weaker compared to perimeter length (Figure 5, Table 2).

Table 2. Log-odds-probability coefficient estimates and p-values from the GLMMs.

	PRS		RAMI		SGA		PTR		ALG		ALOG		TLS	
	β-Est	p-value	β-Est	p-value	β-Est	p-value	β-Est	p-value	β-Est	p-value	β-Est	p-value	β-Est	p-value
Perimeter	0.378	< .001	0.295	< .001	0.425	< .001	0.683	< .001	0.587	< .001	0.899	< .001	0.334	< .001
Surface Area	0.096	< .001	0.021	0.670	0.119	0.010	0.074	0.086	0.111	0.068	-0.104	< .001	0.151	0.001
Interaction	-0.030	< .001	-0.020	< .001	-0.026	< .001	-0.158	< .001	-0.137	< .001	-0.385	< .001	-0.009	0.001
AIC	27621.5		5992.9		5506.1		1661.4		1656		1656		1119.1	

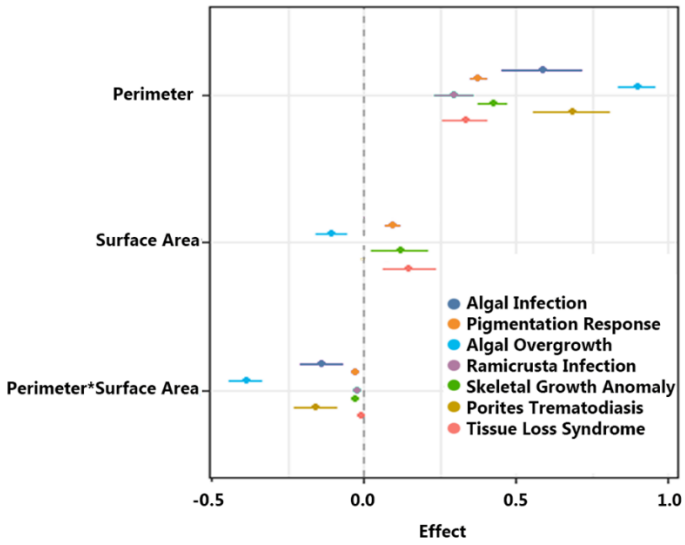

Figure 5. Log-odds-probability coefficient estimates for predictors in GLMMs for seven coral health conditions. Predictor variables were standardized prior to model computations to make log-odds-probability estimates comparable; horizontal lines are 95% confidence intervals. Only significant coefficients were plotted all estimates are reported in Table 2.

The interaction between perimeter and surface area showed interesting trends for the presence of all health conditions (Figure 5). Each of the seven models' likelihood ratio tests indicated that the models with interaction terms revealed that the interaction

between perimeter and surface area of corals provides additional information compared to models without the interaction. With the exception of algal overgrowth and surface area, perimeter and surface area on their own were positive, and the interaction between the two had a negative effect on the presence of each of the health conditions. The interaction term refers to a linear ratio between perimeter length and surface area. The two covariates increasing together causes a net negative effect on the seven health conditions within these data. On contrast, when one of these two variables increases or decreases independently from the other, a positive effect is observed in the models. This was particularly the case for algal overgrowth, algal infection, and *Porites trematodiasis*.

As perimeter length had the largest positive effect for the presence of these health conditions, additional probability curves were created using results from the GLMMs for each health condition to further interpret the results from these analysis (Figure 6). Each of these probability curves suggests that as the perimeter length of a colony increases, the expected probability of having a particular health condition also increases. With health conditions such as algal overgrowth and pigmentation response, smaller colony lengths have a higher expected probability of a health condition being presence. Whereas tissue loss syndrome and *Ramicrusta* infection have high expected probabilities only in colonies with larger perimeters (> 5 m).

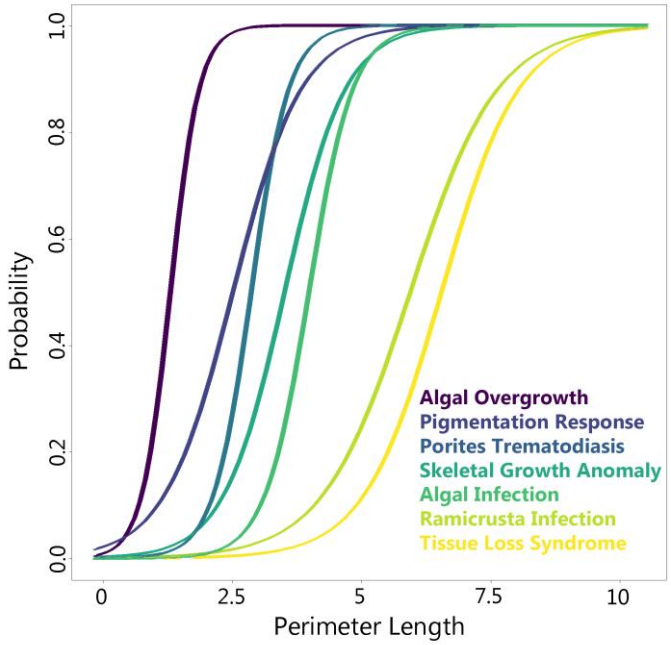

Figure 6. Each curve displays the expected probability of a given health condition based on the perimeter length in meters. Supplementary Figure 5 displays individual graphs for each health condition and site.

Coral Health Reefscape and Colony Spatial Trends

Reefscape- and colony-level spatial assessments of severity revealed interesting trends about the spatial patterns of coral health conditions. *Ramicrusta* infection had the highest percentage of sites (33.3%) where clustered spatial patterning and non-random patterning existed. In contrast, conditions such as algal infection had the lowest number of sites (0.06%) with non-random patterns (Table 3). No one health condition showed spatial clustering at every site surveyed. Skeletal growth anomalies had nine sites (16.6% of sites where present) that had a significant dispersion pattern, suggesting that at these reefscapes skeletal growth anomalies are systematically dispersed among colonies.

Table 3. Finding from Moran's I tests indicating if spatial patterning was present among the seven health conditions assessed. Percent data refers to percent of sites only at which health conditions were present (n = number of sites out of 41). % Sites with clustering refers to the proportion of sites where clustering occurred relative to the sites where the health condition was present. A full description of the site level Moran's I results can be found in Appendix A under Supplementary Table 4.

Health Condition	Sites Present n	% Sites with Clustering	Sites with Clustering n	Sites with Dispersion n	Sites with Random Pattern n	Mean Clustered I Index	Min Clustered I Index	Max Clustered I Index
ALG	15	0.06	1	1	13	0.001	0.001	0.001
PRS	40	22.5	9	0	31	0.007	0.002	0.020
ALOG	41	26.8	11	0	30	0.007	0.001	0.022
RAMI	24	33.3	8	0	16	0.004	0.001	0.036
SGA	36	22.2	8	6	22	0.008	0.001	0.033
PTR	18	11.1	2	2	14	0.002	0.001	0.003
TLS	18	16.6	3	0	15	0.003	0.001	0.005

Local spatial assessments using Getis-Ord local statistics were particularly useful when identifying hotspots of individual health conditions. The G values from the local statistics were mapped onto individual colonies to not only show where colonies in a compromised health state are, but also identify which colonies are within a significant health condition cluster (Figure 7).

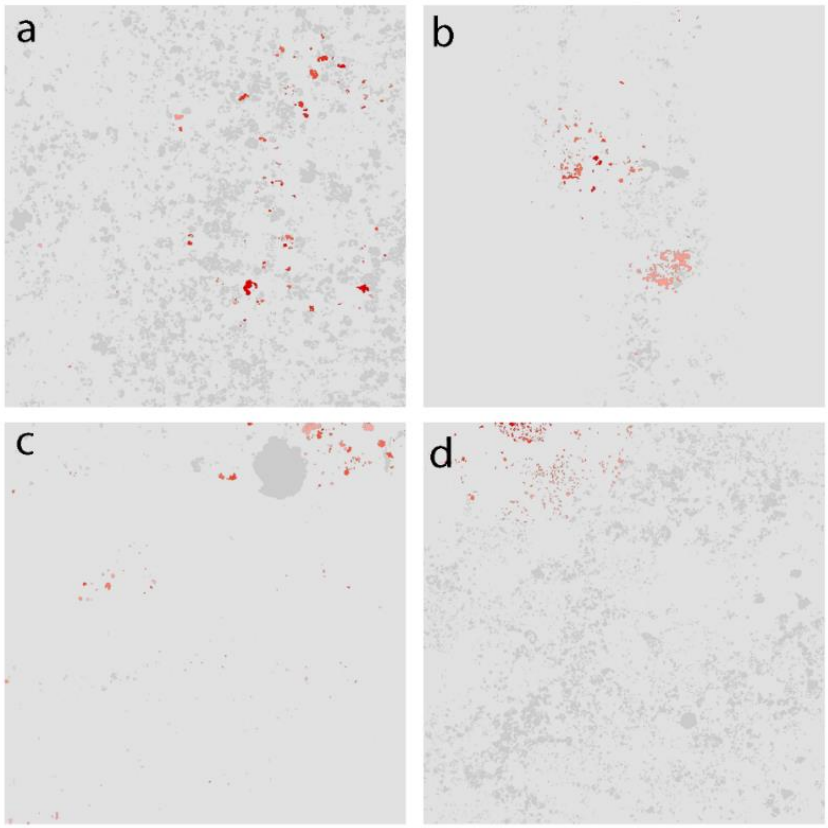

Figure 7. Examples of significant G values from Getis-Ord local statistics mapped onto individual coral colonies. Dark red corals indicate cluster focal points whereas lighter red colors indicate outer sections of hotspot or weaker clusters. Light gray polygons represent individual coral colonies not in health condition clusters but that may still have a health condition. (a) *Ramicrusta* infection, (b) algal overgrowth, (c) pigmentation response, (d) skeletal growth anomalies. The health conditions algal infection, tissue loss syndrome, *Porites* trematodiasis were not included in these local spatial statistics as they did not meet criteria for local statistics.

Discussion

I visually assessed over 100,000 massive *Porites* corals across 41 reefscapes in South Kona, Hawaii to investigate the spatial ecology of individual corals in a health-compromised state. South Kona massive *Porites* corals were observed to have small sizes, loosely clustered spatial patterns, high density, and low size diversity. This suggests that these corals are small, that high recruitment is occurring, and that they are found in loosely clustered assemblages. Attributes representative of colony assemblage structure (spatial pattern, density, diversity in size classes) had little effect on the severity prevalence of health conditions. Surface area and perimeter length proved to be strong indicators for the presence or absence of the seven coral health conditions examined here. Spatial patterning of health condition severity occurred among the seven health conditions, but a random spatial pattern was the dominant pattern observed.

My findings show that when perimeter length and surface area increase together linearly, the effect on the presence of these health conditions is negative. Colony size (diameter) has previously been an indicator of certain conditions such as skeletal growth anomalies and tissue loss syndrome (Caldwell et al., 2020); however, my assessment breaks down colony size into more specific traits. This trend could be representative of the way coral health conditions cause partial mortality on massive *Porites* corals. These corals, when healthy, have radial spherical growth patterns (Sandin et al., 2020;

Forsman et al., 2009). As health conditions cause partial mortality, this morphology may become more obscure and lose its natural spherical shape. This, in turn, can increase the perimeter length and change the surface area to perimeter length ratio. Increased perimeter and surface area proportion suggests larger, rounder, and healthier colonies that have not experienced partial mortality from health conditions. Further hierarchical, multiscale, and temporal investigations into how colony size and trait dynamics relate to health condition presence and colony growth metrics may further reveal this relationship.

By using global and local spatial statistics, I uncovered reefscape- and colony-level spatial patterns of health compromised corals. I found that spatial patterns exist, and that significant clustering and dispersion occur, in health condition severity. However, I found infrequent non-random spatial patterns in most reefs in South Kona. Skeletal growth anomalies was a unique condition in that 39% of the reefs where present exhibited a nonrandom pattern either dispersion or clustering. However, little is known about the cause of skeletal growth anomalies (Burns et al. 2016). The presence of localized spatial structure among colonies due to the severity of a specific condition suggests localized spread of disease (Burns et al., 2016). For three of the health conditions surveyed, localized spread may not be a function of the vectoring of a health condition but could be mediated by the environment or by the biology of individual colonies. Algal overgrowth and pigmentation response were the two most common conditions present and can be the result of a wide range of factors (Couch et al., 2014). The health conditions *Ramicrusta* infection, Algal Infection, and *Porites* Trematodiasis are caused by specific vectors that have potential to move through a reefscape and spread locally or systemically between corals (Aeby 2015).

The use of SfM mosaics to investigate coral health patterns represents a systematic and archivable way to collect spatial data. This form of methodology typically

can yield a wide variety of data that would be impractical to assess *in-situ* during a dive. SfM data sets can be further strengthened when used in temporal studies to measure hundreds of thousands of specific corals, their traits, and their health states through time, something that cannot be achieved via *in-situ* surveys. However, we must recognize that extracting individual health information from detailed mosaics and 3D models may be more challenging than looking at a colony underwater. It is likely that for certain health conditions, skeletal growth anomalies and *Porites* trematodiasis, digital coral health surveys underrepresent the prevalence at which these conditions occur (Burns et al., 2020).

I used polygon centroids as the coordinate for spatial analysis. While this is common in both spatial statistics in all fields and in corals, it skews or biases how close polygons are to one another. Larger colonies have centroids naturally farther from the colony (polygon) edges, whereas smaller colonies have them closer. This creates a differential between colony centroids that may not exist between colony edges and naturally puts larger colonies farther away from its neighboring colonies in the spatial assessment. This may have affected the overall results of the spatial analysis due to the sensitivity of spatial weight matrices. The use of a *MaxdiffK* statistics as the distance between individual colonies at each site may reduce sensitivity in the Moran's I analysis. However, further developments in spatial analysis that use multiple spatial points per coral feature may be the only way to reduce centroid-to-edge bias. This study represents one approach to using spatial matrices when conducting spatial analysis. It is highly likely that different statistical or mathematical approaches when creating spatial matrices such as different Euclidian distances or position weighting would change the overall outcome of the spatial pattern results. Specific to SfM annotations, corals are often not directly touching, and thus spatial matrices commonly used in grids such as rook or

queens' continuity matrices would further bias these resulting I-values. I recommend that future studies, particularly those assessing coral annotations, take caution designing and approaching spatial analysis with these types of data.

First order spatial effects, those relating to external factors or influences that drive spatial patterns, occur among coral spatial data. One of the most common external factors is benthic substrata and corals inability to settle or grow on sand or loose substrates. This creates a bias when assessing spatial patterns of individual coral colonies due to blank spots or areas that are comprised of sand and thus massive *Porites* corals and their coral health conditions are incapable of occurring spatially in these areas. As a result, corals may cluster spatially simply due to limited availability within a given 10 x 10 m area due to or lack of hard substrate. My use of a Global Moran's I assessed the spatial dependence between specific health condition values among colonies rather than the overall spatial pattern of corals. While this does not completely rule out inherent first order effect bias, it may address the issue contextually and provide insight into future studies. My addition of including healthy colonies, those with a severity of 0% for each health condition, into this spatial analysis also aided in reducing the overall influence of these first order effects as it look at all massive *Porites* corals within a site rather than those just in a visibly compromised state.

As research in coral spatial patterns progresses, knowledge gaps still exist. Here, I used large volumes of colony-scale 3D data; however, a surprising lack of statistical frameworks can implement 3D spatial weight matrices. Because of this, I used standard 2D weight matrices. To date, no study has been able to statistically assess the pattern of coral distribution spatially at the colony scale in 3D, due to few spatial statistics using 3D matrices. Previous studies (Pederson et al., 2019; Edwards et al., 2017; Burns et al., 2016) have assessed the spatial pattern of either colony distribution or colony health in

2D, but all (including mine) lacked a statistical approach using a third dimension ($\mathbf{w}_{ij}$ 2D vs $\mathbf{w}_{ijk}$ 3D) in the spatial analysis. New spatial statistics or existing statistics should be further developed to measure 3D spatial clustering to assess the pattern of coral assemblages, disease severity, and growth of corals across 3D reef architecture.

Spatial pattern of both corals and their health conditions are important metrics to assess as reefs change and adapt to future conditions. I implemented a sampling technique that integrated remote sensing data that captured regional habitat variation and combined it with *in-situ* remote sensing using SfM. I examined the relationship of massive *Porites* coral health conditions and their assemblage structure, colony traits, and spatial patterning. I focused on effectiveness of colony traits as predictors for the presence of these health conditions. While I did not detect an effect of assemblage structure on the prevalence or severity of health conditions among corals, this does not necessarily mean no pattern exists. Further investigation and temporal tracking of the spatial distributions of site or reefscape level assemblages in a health compromised state may reveal further trends. The South Kona reefs monitored in this study observed less than 7% of massive *Porites* in a visibly compromised health state, but as conditions change and new diseases spread, understanding ecological spatial patterns of these corals will be critical for coral conservation and determining the spread of diseases. The findings presented here, and the new methodological approaches implemented in this study, can be rapidly applied to existing marine monitoring programs to track the spread of coral health conditions. The addition of a temporal component to these methods may help the predictive capabilities of managing coral health under future conditions. While these methods provide strong archivable and spatial components, evolving them further will allow for increased understandings of the interaction between corals and their surroundings.

REFERENCES

Aeby, G.S., 2015. *Porites* trematodiasis. Diseases of Coral, pp.387-390.

Aeby, G.S., Williams, G.J., Franklin, E.C., Kenyon, J., Cox, E.F., Coles, S. and Work, T.M., 2011. Patterns of coral disease across the Hawaiian archipelago: relating disease to environment. PloS one, 6(5), p.e20370.

Aeby, G.S., 1998. Interactions of the digenetic trematode, Podocotyloides stenometra, with its coral intermediate host and butterflyfish definitive host: ecology and evolutionary implications. University of Hawai'i at Manoa.

Asner, G.P., Vaughn, N., Grady, B.W., Foo, S.A., Anand, H., Carlson, R.R., Shafron, E., Teague, C. and Martin, R.E., 2021. Regional Reef Fish Survey Design and Scaling Using High-Resolution Mapping and Analysis. Frontiers in Marine Science, p.894

Asner, G.P., Vaughn, N.R., Heckler, J., Knapp, D.E., Balzotti, C., Shafron, E., Martin, R.E., Neilson, B.J. and Gove, J.M., 2020 . Large-scale mapping of live corals to guide reef conservation. Proceedings of the National Academy of Sciences, 117(52), pp.33711-33718.

Bayley, D.T. and Mogg, A.O., 2020. A protocol for the large-scale analysis of reefs using Structure from Motion photogrammetry. Methods in Ecology and Evolution, 11(11), pp.1410-1420.

Bryson, M., Ferrari, R., Figueira, W., Pizarro, O., Madin, J., Williams, S., et al. (2017). Characterization of measurement errors using structure-from-motion and photogrammetry to measure marine habitat structural complexity. Ecol. Evol. 7, 5669–5681. doi: 10.1002/ece3.3127

Burns, J.H., Weyenberg, G., Mandel, T., Ferreira, S.B., Gotshalk, D., Kinoshita, C.K., Marshall, M.J., Del Moral, N.A., Murphy, S.J., Pascoe, K.H. and Runyan, A., 2020. A comparison of the diagnostic accuracy of in-situ and digital image-based assessments of coral health and disease. Frontiers in Marine Science, 7, p.304.

Burns, J.H., Alexandrov, T., Ovchinnikova, E., Gates, R.D. and Takabayashi, M., 2016. Investigating the spatial distribution of growth anomalies affecting Montipora capitata corals in a 3-dimensional framework. Journal of invertebrate pathology, 140, pp.51-57.

Burns, J.H.R., Delparte, D., Gates, R.D. and Takabayashi, M., 2015. Integrating structure-from-motion photogrammetry with geospatial software as a novel technique for quantifying 3D ecological characteristics of coral reefs. PeerJ, 3, p.e1077.

Burns, J.H.R., Rozet, N.K. and Takabayashi, M., 2011. Morphology, severity, and distribution of growth anomalies in the coral, Montipora capitata, at Wai ʻōpae, Hawai ʻi. Coral reefs, 30(3), pp.819-826.

Caldwell, J.M., Aeby, G., Heron, S.F. and Donahue, M.J., 2020. Case-control design identifies ecological drivers of endemic coral diseases. Scientific reports, 10(1), pp.1-11.

Caldwell, J.M., Heron, S.F., Eakin, C.M. and Donahue, M.J., 2016. Satellite SST-based coral disease outbreak predictions for the Hawaiian archipelago. Remote sensing, 8(2), p.93.

Chen, Z., Scott, T.R., Bearman, S., Anand, H., Keating, D., Scott, C., Arrowsmith, J.R. and Das, J., 2019. Geomorphological Analysis Using Unpiloted Aircraft Systems, Structure from Motion, and Deep Learning. arXiv preprint arXiv:1909.12874.

Couch, C., Suka, R., Oliver, T., Lamirand, M., Asbury, M., Amir, C., Vargas-Angel, B., Winston, M., Huntington, B., Lichowski, F. and Halperin, A., 2021. Comparing coral demographic surveys from in situ observations and Structure-from-Motion imagery shows low methodological bias.

Couch, C.S., Burns, J.H., Liu, G., Steward, K., Gutlay, T.N., Kenyon, J., Eakin, C.M. and Kosaki, R.K., 2017. Mass coral bleaching due to unprecedented marine heatwave in Papahānaumokuākea Marine National Monument (Northwestern Hawaiian Islands). PloS one, 12(9), p.e0185121.

Couch, C.S., Garriques, J.D., Barnett, C., Preskitt, L., Cotton, S., Giddens, J. and Walsh, W., 2014. Spatial and temporal patterns of coral health and disease along leeward Hawai'i Island. Coral Reefs, 33(3), pp.693-704.

Edmunds, P.J. and Riegl, B., 2020. Urgent need for coral demography in a world where corals are disappearing. Marine Ecology Progress Series, 635, pp.233-242.

Edwards, C.B., Eynaud, Y., Williams, G.J., Pedersen, N.E., Zgliczynski, B.J., Gleason, A.C., Smith, J.E. and Sandin, S.A., 2017. Large-area imaging reveals biologically driven non-random spatial patterns of corals at a remote reef. Coral Reefs, 36(4), pp.1291-1305.

Ferrari, R., Figueira, W. F., Pratchett, M. S., Boube, T., Adam, A., KobelkowskyVidrio, T., et al. (2017). 3D photogrammetry quantifies growth and external erosion of individual coral colonies and skeletons. Sci. Rep. 7:16737. doi: 10. 1038/s41598-017-16408-z

Forsman, Z.H., Barshis, D.J., Hunter, C.L. and Toonen, R.J., 2009. Shape-shifting corals: molecular markers show morphology is evolutionarily plastic in *Porites*. *BMC evolutionary biology*, *9*(1), pp.1-9.

Fox, M. D., Carter, A. L., Edwards, C. B., Takeshita, Y., Johnson, M. D., Petrovic, V., et al. (2019). Limited coral mortality following acute thermal stress and widespread bleaching on Palmyra Atoll, central Pacific. Coral Reefs 38, 701–712. doi: 10.1007/s00338-019-01796-7

Harvell, D., Jordán-Dahlgren, E., Merkel, S., Rosenberg, E., Raymundo, L., Smith, G., Weil, E. and Willis, B., 2007. Coral disease, environmental drivers, and the balance between coral and microbial associates. Oceanography, 20, pp.172-195.

Magel, J.M., Burns, J.H., Gates, R.D. and Baum, J.K., 2019. Effects of bleaching-associated mass coral mortality on reef structural complexity across a gradient of local disturbance. Scientific reports, 9(1), pp.1-12.

Maynard, J., Van Hooidonk, R., Eakin, C.M., Puotinen, M., Garren, M., Williams, G., Heron, S.F., Lamb, J., Weil, E., Willis, B. and Harvell, C.D., 2015. Projections of climate conditions that increase coral disease susceptibility and pathogen abundance and virulence. Nature Climate Change, 5(7), pp.688-694.

McKay, M.D., Beckman, R.J. and Conover, W.J., 2000. A comparison of three methods for selecting values of input variables in the analysis of output from a computer code. Technometrics, 42(1), pp.55-61.

Miller, J., Muller, E., Rogers, C., Waara, R., Atkinson, A., Whelan, K.R.T., Patterson, M. and Witcher, B., 2009. Coral disease following massive bleaching in 2005 causes 60% decline in coral cover on reefs in the US Virgin Islands. Coral Reefs, 28(4), p.925.

Montilla, L.M., Ascanio, A., Verde, A. and Croquer, A., 2019. Systematic review and meta-analysis of 50 years of coral disease research visualized through the scope of network theory. PeerJ, 7, p.e7041.

Moran, P.A., 1950. Notes on continuous stochastic phenomena. Biometrika, 37(1/2), pp.17-23.

Muller, E.M., Sartor, C., Alcaraz, N.I. and van Woesik, R., 2020. Spatial epidemiology of the stony-coral-tissue-loss disease in Florida. Frontiers in Marine Science, 7, p.163.

Nicolet, K.J., 2017. Vectors and environmental drivers of coral disease dynamics on the Great Barrier Reef (Doctoral dissertation, James Cook University).

Ord, J.K. and Getis, A., 1995. Local spatial autocorrelation statistics: distributional issues and an application. *Geographical analysis*, *27*(4), pp.286-306.

Pascoe, K.H., Fukunaga, A., Kosaki, R.K. and Burns, J.H., 2021. 3D assessment of a coral reef at Lalo Atoll reveals varying responses of habitat metrics following a catastrophic hurricane. Scientific reports, 11(1), pp.1-9.

Patterson, K.L., Porter, J.W., Ritchie, K.B., Polson, S.W., Mueller, E., Peters, E.C., Santavy, D.L. and Smith, G.W., 2002. The etiology of white pox, a lethal disease of the Caribbean elkhorn coral, Acropora palmata. Proceedings of the National Academy of Sciences, 99(13), pp.8725-8730.

Pavoni, G., Corsini, M., Pedersen, N., Petrovic, V. and Cignoni, P., 2020. Challenges in the deep learning-based semantic segmentation of benthic communities from Ortho-images. Applied Geomatics, pp.1-16.

Pedersen, N. E., Edwards, C. B., Eynaud, Y., Gleason, A. C. R., Smith, J. E., & Sandin, S. A. (2019). The influence of habitat and adults on the spatial distribution of juvenile corals. Ecography. doi: 10.1111/ecog.04520

Richardson, L.L., Goldberg, W.M., Kuta, K.G., Aronson, R.B., Smith, G.W., Ritchie, K.B., Halas, J.C., Feingold, J.S. and Miller, S.L., 1998. Florida's mystery coral-killer identified. Nature, 392(6676), pp.557-558.

Ruiz-Moreno, D., Willis, B.L., Page, A.C., Weil, E., Cróquer, A., Vargas-Angel, B., Jordan-Garza, A.G., Jordán-Dahlgren, E., Raymundo, L. and Harvell, C.D., 2012. Global coral disease prevalence associated with sea temperature anomalies and local factors. Diseases of aquatic organisms, 100(3), pp.249-261.

Sheridan, C., Baele, J.M., Kushmaro, A., Frejaville, Y. and Eeckhaut, I., 2014. Terrestrial runoff influences white syndrome prevalence in SW Madagascar. Marine environmental research, 101, pp.44-51.

Sherwood, A.R., Paiano, M.O., Wade, R.M., Cabrera, F.C., Spalding, H.L. and Kosaki, R.K., (2021) a. Biodiversity of Hawaiian Peyssonneliales (Rhodophyta). 1. Two new species in the genus Ramicrusta from Lehua Island. Pacific Science, 75(2), pp.185-195. https://doi.org/10.2984/75.2.2

Sandin, S.A., Edwards, C.B., Pedersen, N.E., Petrovic, V., Pavoni, G., Alcantar, E., Chancellor, K.S., Fox, M.D., Stallings, B., Sullivan, C.J. and Rotjan, R.D., 2020. Considering the rates of growth in two taxa of coral across Pacific islands. In *Advances in Marine Biology* (Vol. 87, No. 1, pp. 167-191). Academic Press.

Thurber, R.V., Mydlarz, L.D., Brandt, M., Harvell, D., Weil, E., Raymundo, L., Willis, B.L., Langevin, S., Tracy, A.M., Littman10, R. and Kemp11, K.M., 2020. Deciphering Coral Disease Dynamics: Integrating Host, Microbiome, and the Changing Environment. Frontiers in Ecology and Evolution, 8.

Walsh, W., Cotton, S., Barnett, C., Couch, C., Preskitt, L., Tissot, B. and Osada-D'Avella, K., 2013. Long-term monitoring of coral reefs of the main Hawaiian Islands. NOAA Coral Reef Conservation Program, Hawai'i Division of Aquatic Resources.

Ward, J.R., Kim, K. and Harvell, C.D., 2007. Temperature affects coral disease resistance and pathogen growth. Marine Ecology Progress Series, 329, pp.115-121.

Winston, M., Couch, C.S., Ferguson, M., Huntington, B., Swanson, D.W. and Vargas-Ángel, B., 2019. Ecosystem sciences division standard operating procedures: Data collection for rapid ecological assessment benthic surveys, 2018 update.

Work, T. and Meteyer, C., 2014. To understand coral disease, look at coral cells. EcoHealth, 11(4), pp.610-618.

Yoshioka, R.M., Kim, C.J., Tracy, A.M., Most, R. and Harvell, C.D., 2016. Linking sewage pollution and water quality to spatial patterns of *Porites* lobata growth anomalies in Puako, Hawaii. Marine pollution bulletin, 104(1-2), pp.313-321.

Young, B.D., Serrano, X.M., Rosales, S.M., Miller, M.W., Williams, D. and Traylor-Knowles, N., 2020. Innate immune gene expression in Acropora palmata is consistent despite variance in yearly disease events. Plos one, 15(10), p.e0228514.

APPENDIX A

SUPPLEMENTARY FILES

Massive *Porites* Site Reduction Data

We used four metrics that describe massive *Porites* spatial distribution and colony characteristics at each site: colony density, size class diversity, average colony size (m^2), and a site level spatial index. We quantified colony density by the (n) number of colonies divided by the total survey area to measure colonies m^2. Size class diversity uses a coral size binning system commonly used in coral health surveys (Aeby 2006), using the longest axis of a coral colony as colony size. Each coral colony is placed in one of the following bins: (a) 0-5 cm, (b) 5-10 cm, (c) 10-20 cm, (d) 20-40 cm, (e) 40-80 cm, (f) 80-160 cm, or (g) >160 cm. Each size class is used to calculate the Shannon Diversity Index (Shannon 1958) to capture the diversity of sizes that occurs at each site. This index is a combination of alpha diversity and evenness and aims to assess the range and distribution of coral sizes at a site. Average colony size is calculated by using the mean 2D polygon surface area. The spatial index is determined by using a Global Moran's I test and using the Moran's Index statistic as an indicator for spatial patterning. An index at or nearer 1 indicates a site with highly clustered corals, at or near 0 indicates a random distribution, and at or nearer -1 indicates highly dispersed corals. A Ripley's K statistic using site coral annotations was conducted to calculate the *MaxdiffK* statistic. The *MaxdiffK* is the maximum differential at which spatial structuring occurs compared to 100 theoretical permutations or configurations (Burns et al., 2016). We use the *MaxdiffK* statistic as the Euclidean distance in the specified bandwidth for the Global Moran's I test to test for spatial autocorrelation and determine the spatial index at each site as well as for all site level spatial analysis.

Descriptions of surveyed coral diseases and health conditions

Algal Infection (ALG) is the cause of filamentous algae directly growing onto live coral tissue. This direct infiltration often causes polyp stress which may lead to pigmentation response or partial mortality

Pigmentation response (PRS) like that sub-acute tissue loss can be caused by several various causes and sources. Pigmentation Response is the creation of a fluorescent protein in response to a stressor at or around an afflicted area (Kubomura et al., 2021) that can be present across an entire colony or localized to one area.

Algal Overgrowth (ALOG) refers to the presence of any algae that is actively overgrowing or smothering coral colonies and causes direct harm/abrasion/injury/response to tissue.

Ramicrusta Infection (RAMI) is a form of algal overgrowth/infection where algae of the genera *Ramicrusta* can be seen overgrowing/infecting the live tissue of a given colony. Unlike many algae, *Ramicrusta* spp. can readily overtake coral colonies, smothering and killing live coral tissue.

Skeletal growth anomalies (SGA) are a health condition that is the hyperplasia of the corallite structure in each colony and prevents normal cellular and biological function such as feeding, reproduction, defense, and lipid production (Burns et al 2016., Burns and Takabayashi 2011; Sale et al., 2019).

Porites Trematodiasis (PTR) is a health condition that influences only the genus *Porites* and is caused by parasitic trematode and forms a metacercarial cyst in the gastrovascular cavity within the polyp's tentacles of *Porites spp* (Aeby 2015; Aeby 1998). The result is the infected tissue that is unable to feed, the production of enzymes creating a pigmentation response, and an increase in nematocysts requiring further energy production (Aeby 1998).

Tissue Loss Syndrome (TLS) is a generalization term that refers to a condition where a loss of tissue takes place at a progressive rate and could be the cause of any number of sources (Winston et al., 2018).

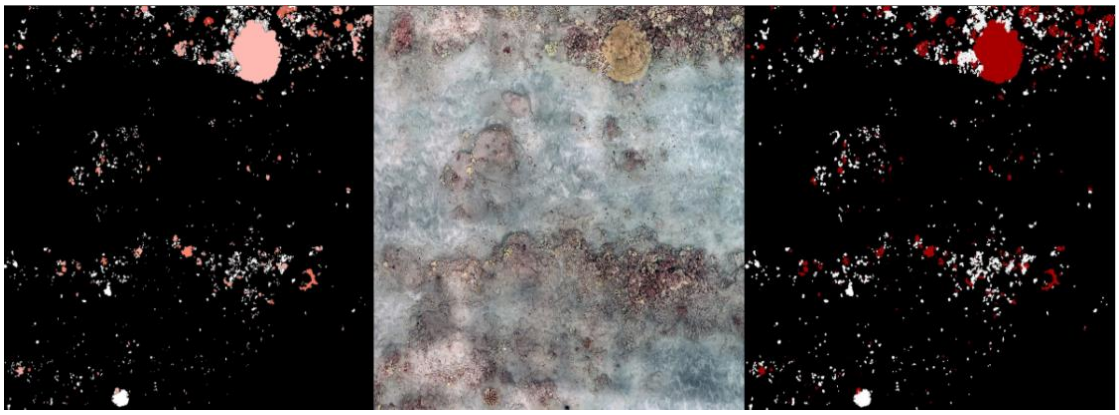

Supplementary Figure 1. Examples of orthomosaic (Center), coral annotations with severity levels (Left), and coral annotations with presence or absence of a compromised health state (Right).

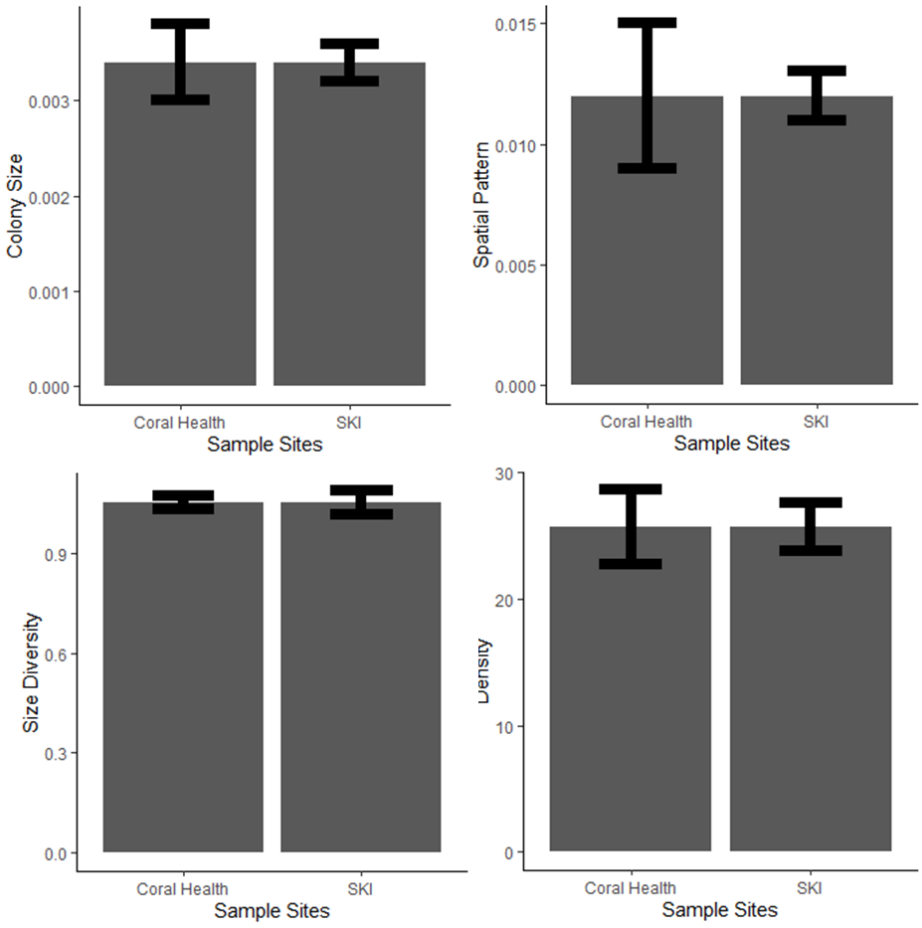

Supplementary Figure 2. Comparisons of mean and standard error values for the four coral assemblage structure variables from the original SKI sites and the subset coral health survey sites.

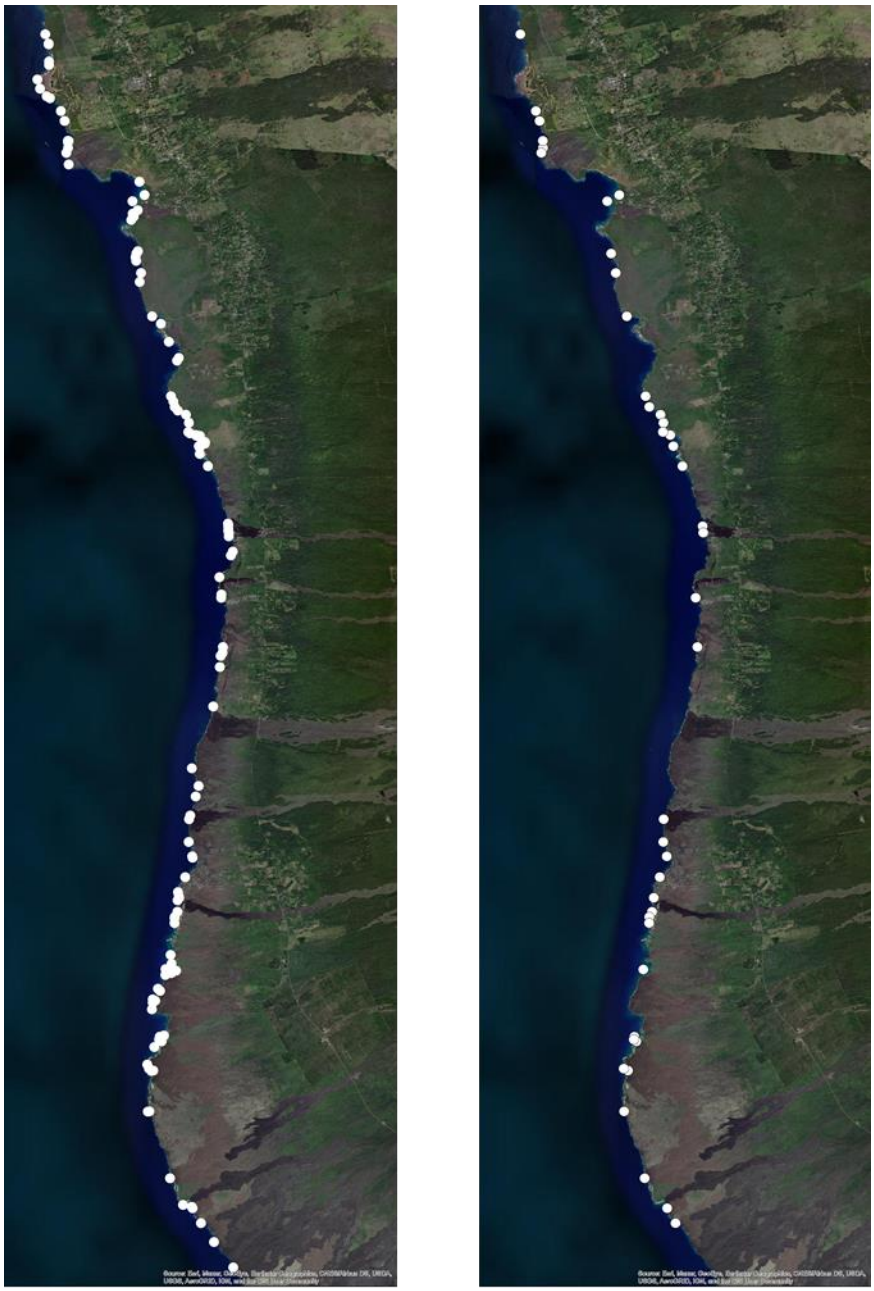

Supplementary Figure 3. Map Of South Kona Intensive Study sites (Left) and map of 41subsetted sites that coral health surveys were conducted at.

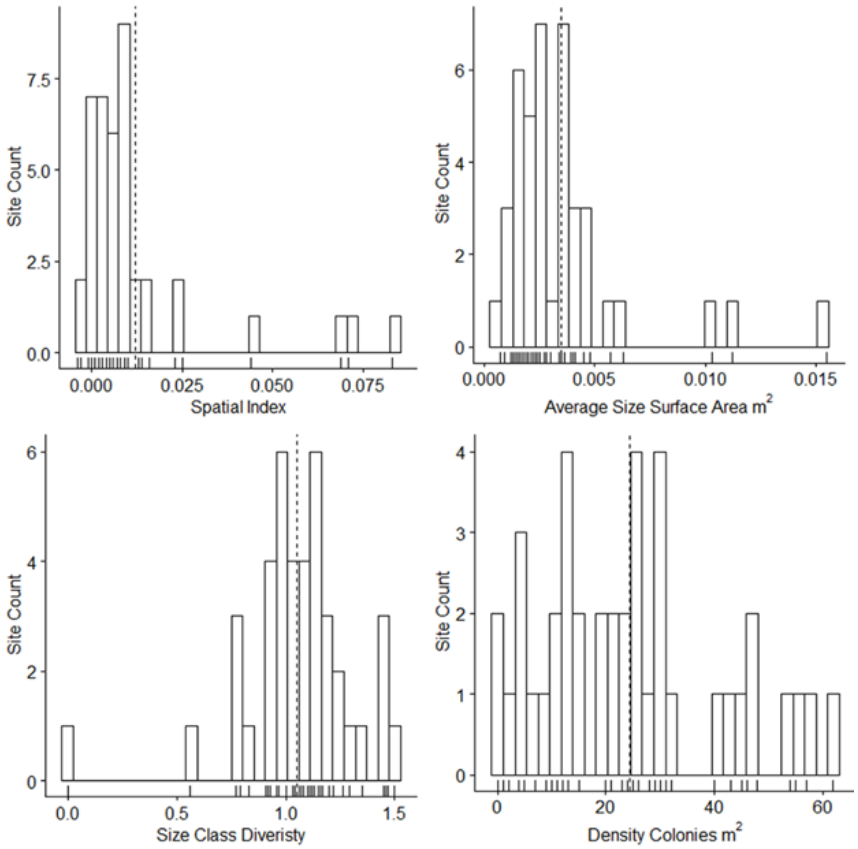

Supplementary Figure 4. Distribution of the assemblage structure variables summarized to site level means: spatial index (Top Left), average size (Top Right), size class diversity (Bottom Left), density (Bottom Right). Dotted line signifies variable mean.

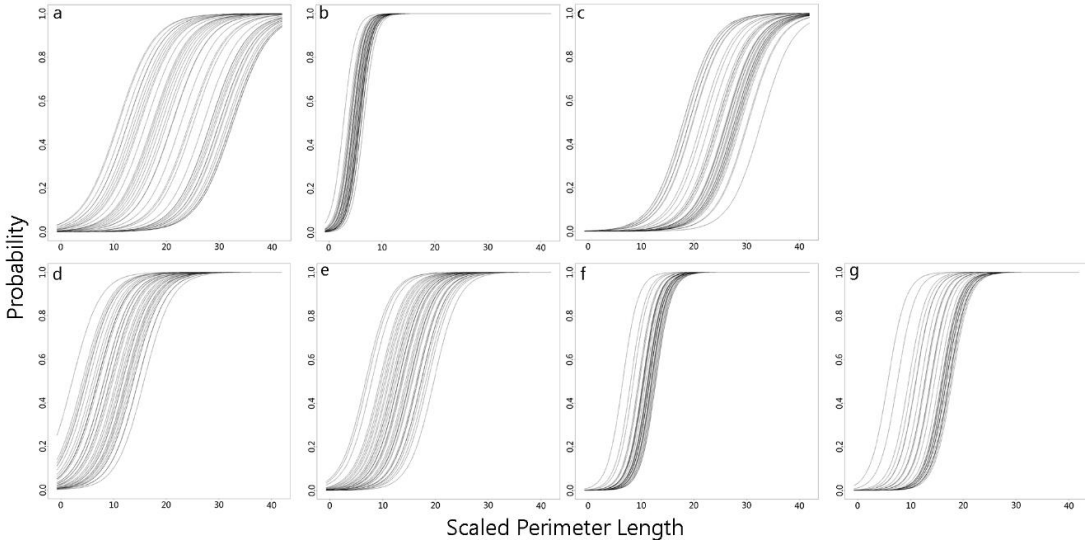

Supplementary Figure 5. Probability curves where each line represents a sites probability curve for a health condition and perimeter length. (a) Ramicrusta Infection, (b) Algal Overgrowth, (c) Tissue Loss Syndrome (image pending), (d) Pigmentation Response, (e) Skeletal Growth Anomalies, (f) Porites Trematodiasis, and (g) Algal Infection.

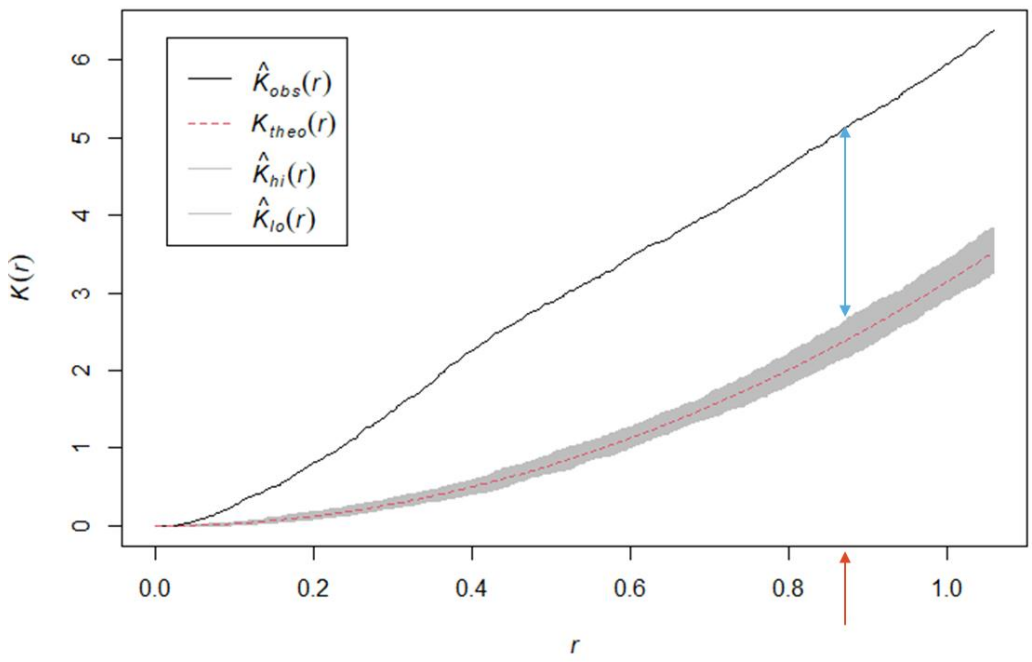

Supplementary Figure 6. Graphical results of Ripley's K statistic from an example SKI site. Grey envelope indicates the distribution of 100 theoretical permutations of corals for the example site, red dashed line indicates the average theoretical observed spatial pattern, and the thicker black line indicates the observed spatial pattern and the given radius (r). The Blue Arrows indicate the *MaxdiffK* Statistic, and the red arrow indicates the radius at which the maximum differential of observed spatial clustering occurs among corals at this site.

Supplementary Table 1. Table of South Kona Intensive sites used and individual site variables for hypercube sampling. Reduction percentile bins one, two, and three are also included.

	***Porites* Massive Assemblage Variables**				**Percentile Bins**			
Site	Colony Size I-Index	Average Colony Size m^2	Colony Density m^2	Size Class Diversity	Colony Size I-Index	Average Colony Size m^2	Colony Density m^2	Size Class Diversity
5	0.025	0.0035	24	1.17	3	2	2	3
6	0.01	0.0027	55	1.12	3	2	3	2
9	0.071	0.0045	0	1.16	3	3	1	3
13	0.023	0.0009	4	0.77	3	1	1	1
15	0.005	0.0024	28	1.07	2	2	2	2
17	0.01	0.0017	5	1	3	1	1	2
19	0.006	0.003	23	1.15	2	2	2	3
20	0.044	0.0016	21	0.97	3	1	2	2
21	0.008	0.0022	57	1.04	2	2	3	2
25	-0.001	0.0014	9	0.91	1	1	1	1
28	0	0.0039	10	1.06	1	3	1	2
34	0.001	0.0023	29	1.03	1	2	2	2
38	0.007	0.0012	43	0.79	2	1	3	1
40	0.016	0.0112	26	1.5	3	3	2	3
45	-0.004	0.0063	7	1.35	1	3	1	3
55	0.013	0.0045	46	1.22	3	3	3	3
60	0.013	0.0013	54	0.83	3	1	3	1
62	0.006	0.0015	20	0.92	2	1	2	1
68	0.006	0.0057	26	1.29	2	3	2	3
101	0.014	0.0021	20	0.97	3	2	2	2
106	0.009	0.0048	31	1.26	2	3	3	3
108	0.069	0.0025	1	1.1	3	2	1	2
109	0.003	0.0014	21	0.91	1	1	2	1
111	0.009	0.0155	5	1.46	2	3	1	3
121	0.002	0.0019	26	0.96	1	2	1	2
122	0.004	0.0025	45	1.03	1	1	3	1
129	-0.001	0.0027	25	0.96	1	2	3	2
132	-0.003	0.0034	12	0.93	1	2	2	1
136	0.009	0.002	13	0.97	1	2	1	1
138	0.009	0.0012	11	0.79	2	1	1	2
145	0.009	0.0007	12	0.56	2	1	1	1
146	0.003	0.0028	40	0	1	2	3	1
148	0.008	0.0018	31	1.47	2	1	3	3
151	0.001	0.0036	32	1.13	1	3	3	2
153	0.005	0.004	62	1.11	2	3	3	2
154	0.001	0.0041	30	1.13	1	3	2	2
169	0.083	0.0036	2	1.08	3	3	1	2
170	0.002	0.0103	15	1.45	1	3	2	3
173	0.001	0.0035	13	1.2	1	2	1	3
175	0.002	0.0036	48	1.17	1	3	3	3
176	0.004	0.0034	15	1.16	1	2	2	3

Supplementary Table 2. Finding from OLS multiple regressions assessing trends between individual health condition proportional severity and site level assemblage variables. Reported below are the coefficient estimates and p-value for each covariate, and overall model p-value and adjusted R^2.

	ALG		**PRS**		**ALOG**		**RAMI**		**SGA**		**PTR**		**TLS**	
	β-Est	**p-value**	**β-Est**	**p-value**	**β-Est**	**p-value**	**β-Est**	**p-value**	**β-Est**	**p-value**	**β-Est**	**p-value**	**β-Est**	**p-value**
Colony Density	0.165	0.268	0.047	0.530	0.081	0.183	-0.031	0.838	-0.165	0.107	0.001	0.960	**0.597**	**0.003**
Size Class Diversity	0.097	0.483	0.011	0.876	-0.034	0.540	-0.254	0.088	0.149	0.146	**0.059**	**0.036**	0.053	0.767
Spatial Index	0.175	0.242	0.048	0.521	-0.105	0.088	-0.194	0.216	0.113	0.236	0.006	0.793	-0.174	0.366
p-value	0.235		0.737		0.058		0.198		0.049		0.158		0.006	
Adj-R^2	0.034		-0.045		0.114		0.045		0.123		0.058		0.223	

Supplementary Table 3. Finding from OLS multiple regressions assessing trends between individual health condition prevalence per 1000 *Porites* massive colonies and site level assemblage variables. Reported below are the coefficient estimates and p-value for each covariate, and overall model p-value and adjusted R^2.

	ALG		PRS		ALOG		RAMI		SGA		PTR		TLS	
	β-Est	**p-value**	**β-Est**	**p-value**	**β-Est**	**p-value**	**β-Est**	**p-value**	**β-Est**	**p-value**	**β-Est**	**p-value**	**β-Est**	**p-value**
Colony Density	-2.104	0.271	-20.457	0.074	-2.288	0.313	-2.104	0.271	**-7.499**	**0.010**	-0.077	0.887	0.124	0.502
Size Class Diversity	-0.912	0.608	2.3744	0.821	-2.698	0.350	-0.912	0.608	**7.095**	**0.009**	0.748	0.150	0.104	0.546
Spatial Index	-0.946	0.618	0.220	0.984	2.119	0.205	-0.946	0.618	-0.901	0.747	0.470	0.393	-0.218	0.241
p-value	0.679		0.284		0.222		0.679		0.004		0.378		0.385	
Adj-R^2	-0.038		0.022		0.038		-0.038		0.236		0.004		0.003	

Supplementary Table 4. Finding from Moran's I test indicating if spatial patterning was present among the seven health conditions assessed.

	Ramicrusta Overgrowth		Pigmentation Response		Skeletal Growth Anomalies		*Porites* Trematodiasis		Algal Infection		Algal Overgrowth		Tissue Loss Syndrome	
Site	**P-value**	**I Index**	**P-value**	**I Index**	**P-value**	**I Index**	**P-value**	**I Index**	**P-value**	**I Index**	**P-value**	**I Index**	**P-value**	**I Index**
5	-	-	**0.025**	0.0058	0.140	-0.0004	**0.050**	0.0033	0.305	-0.0007	**0.040**	0.0048	-	-
6	-	-	0.110	0.0006	0.455	-0.0003	0.495	-0.0003	-	-	0.075	0.0006	0.085	0.0006
9	-	-	0.325	-0.0175	**0.020**	-0.0400	-	-	-	-	0.110	-0.0430	-	-
13	-	-	0.485	-0.0040	**0.045**	0.0144	-	-	-	-	**0.040**	0.0222	-	-
15	**0.005**	0.0044	**0.020**	0.0031	0.460	-0.0004	**0.040**	-0.0012	-	-	**0.025**	0.0017	0.085	-0.0007
17	0.350	-0.0011	**0.015**	0.0206	0.380	-0.0021	-	-	-	-	0.305	-0.0040	-	-
19	-	-	0.050	0.0013	0.095	-0.0014	0.060	-0.0005	**0.025**	-0.0006	0.485	-0.0008	-	-
20	-	-	0.405	-0.0004	0.105	0.0015	0.350	-0.0005	-	-	0.255	0.0004	-	-
21	-	-	**0.005**	0.0026	**0.005**	0.0047	0.245	-0.0002	-	-	0.180	0.0003	**0.020**	0.0013
25	-	-	0.115	0.0021	0.455	-0.0014	0.470	-0.0011	-	-	0.255	0.0005	-	-
28	-	-	**0.030**	0.0093	**0.030**	0.0067	0.175	-0.0017	-	-	0.050	0.0052	0.170	0.0013
34	**0.030**	0.0016	0.220	-0.0014	0.350	0.0000	0.280	-0.0003	**0.050**	0.0010	0.195	-0.0013	-	-
38	**0.005**	0.0016	**0.005**	0.0049	**0.010**	0.0023	**0.035**	0.0017	-	-	0.075	0.0010	-	-
40	-	-	0.145	0.0009	**0.040**	-0.0019	-	-	-	-	0.055	0.0023	-	-
45	-	-	0.485	-0.0020	**0.005**	0.0330	0.475	-0.0022	0.230	-0.0023	**0.010**	0.0197	-	-
55	-	-	0.135	0.0007	**0.005**	0.0034	0.215	0.0002	0.290	-0.0005	**0.025**	0.0017	0.290	0.0000
60	-	-	**0.005**	0.0060	-	-		-	-	-	**0.005**	0.0069	-	-
62	**0.005**	0.0081	**0.005**	0.0083	**0.035**	0.0034	-	-	-	-	0.475	-0.0009	0.415	-0.0012
68	0.305	0.0002	0.085	0.0010	0.165	0.0003	-	-	-	-	0.270	0.0000	-	-
101	-	-	0.195	-0.0015	0.225	0.0005	-	-	-	-	0.085	0.0016	-	-
106	-	-	0.235	0.0050	**0.035**	-0.0012	0.435	-0.0005	0.480	-0.0003	**0.005**	0.0027	0.370	-0.0007
108	0.325	-0.0203	-	-	-	-	-	-	-	-	0.370	-0.0125	-	-
109	0.265	-0.0011	0.345	-0.0013	0.250	0.0002	-	-	-	-	0.095	0.0018	-	-
111	-	-	0.060	0.0099	0.470	-0.0036	-	-	-	-	0.220	-0.0010	-	-
121	0.110	0.0011	0.320	0.0001	**0.005**	-0.0002	-	-	0.055	-0.0005	0.090	0.0022	0.105	0.0009
122	0.380	-0.0001	0.100	0.0004	0.500	-0.0003	-	-	0.095	0.0006	0.360	0.0000	0.240	-0.0003
129	0.430	-0.0003	**0.005**	0.0052	0.220	0.0004	-	-	0.400	-0.0008	**0.005**	0.0072	0.205	-0.0004
132	0.435	-0.0007	0.372	-0.0016	-	-	-	-	0.160	0.0013	0.445	-0.0009	-	-
136	**0.010**	0.0077	0.125	-0.0024	-	-	-	-	0.305	-0.0007	**0.035**	0.0051	-	-
138	0.090	0.0021	0.445	0.0014	-	-	-	-	-	-	**0.015**	0.0086	-	-
145	0.170	0.0010	0.145	0.0009	0.405	0.0008	-	-	0.135	-0.0025	0.195	-0.0025	-	-
146	0.175	0.0001	0.445	-0.0005	0.065	-0.0002	0.470	-0.0003	-	-	**0.035**	0.0015	0.475	-0.0004
148	**0.045**	0.0021	0.480	-0.0004	**0.015**	-0.0008	**0.035**	-0.0002	0.150	-0.0004	0.295	0.0002	0.060	-0.0004
151	**0.005**	0.0039	0.270	-0.0009	0.305	0.0000	-	-	-	-	0.090	0.0012	**0.005**	0.0055
153	0.255	0.0001	0.475	-0.0001	**0.015**	0.0016	0.410	-0.0004	0.245	-0.0001	0.190	0.0003	**0.005**	0.0021
154	0.110	0.0006	0.380	-0.0020	0.325	0.0000	0.205	-0.0004	-	-	0.465	-0.0005	-	-
169	0.450	-0.0066	0.440	-0.0073	0.175	0.0063	0.405	-0.0069	-	-	0.245	0.0048	-	-
170	0.305	-0.0019	0.205	-0.0015	0.390	-0.0040	-	-	-	-	0.125	0.0018	0.405	-0.0007
173	-	-	0.490	-0.0011	0.185	0.0012	-	-	-	-	0.110	0.0022	0.255	-0.0007
175	**0.005**	0.0068	0.065	0.0010	**0.035**	-0.0008	-	-	0.375	-0.0001	0.340	-0.0001	0.450	-0.0002
176	0.220	0.0006	0.330	-0.0010	0.115	-0.0022	-	-	-	-	0.065	0.0017	0.330	-0.0007